Efficient Energy Transfer and Electron Transfer in an Artificial Photosynthetic Antenna−Reaction Center Complex†

Gerdenis Kodis,[#] Paul A. Liddell,[#] Linda de la Garza,[#] P. Christian Clausen,[§] Jonathan S. Lindsey,*[,§] Ana L. Moore,*[,#] Thomas A. Moore,*[,#] and Devens Gust*[,#]

Department of Chemistry and Biochemistry, Arizona State University, Tempe, Arizona 85287, and Department of Chemistry, North Carolina State University, Raleigh, North Carolina 27695

Received: June 5, 2001; In Final Form: November 19, 2001

A highly efficient functional mimic of a photosynthetic antenna−reaction center complex has been designed, synthesized, and studied spectroscopically. The antenna, consisting of four covalently linked zinc tetraarylporphyrins, $(P_{ZP})_3-P_{ZC}$, has been coupled to a free-base porphyrin−fullerene artificial photosynthetic reaction center, $P-C_{60}$, to form a $(P_{ZP})_3-P_{ZC}-P-C_{60}$ hexad. As revealed by time-resolved absorption and emission studies in 2-methyltetrahydrofuran solution at ambient temperature, excitation of a peripheral zinc porphyrin moiety is followed by singlet−singlet energy transfer to the central zinc porphyrin to give $(P_{ZP})_3-{}^1P_{ZC}-P-C_{60}$ with a time constant of 50 ps. The excitation is passed on to the free-base porphyrin in 32 ps to produce $(P_{ZP})_3-P_{ZC}-{}^1P-C_{60}$, which decays by electron transfer to the fullerene with a time constant of 25 ps. The resulting $(P_{ZP})_3-P_{ZC}-P^{\bullet+}-C_{60}^{\bullet-}$ charge-separated state is generated with a quantum yield of 0.98 based on light absorbed by the porphyrin antenna. Direct excitation of the free-base porphyrin moiety or the fullerene also generates this state with a yield near unity. Thermodynamically favorable migration of positive charge into the zinc porphyrin array transforms the initial state into a long-lived $((P_{ZP})_3-P_{ZC})^{\bullet+}-P-C_{60}^{\bullet-}$ charge-separated state with a time constant of 380 ps. The final charge-separated state, formed in high yield (∼0.90), decays to the ground state with a lifetime of 240 ns. In benzonitrile, the lifetime is 25 μs. A previous hexad, which differs from the current hexad solely in the nature of the free-base porphyrin, gave a charge-separated state with a lower yield (0.69) and a shorter lifetime (1.3 ns). The difference in performance is attributed to differences in electronic composition (a_{2u} versus a_{1u} HOMO), conformation, and oxidation potential (1.05 versus 0.84 V) between the *meso*-tetraarylporphyrin and the β-octaalkylporphyrin of the current and former hexads, respectively. These results can be explained on the basis of an understanding of factors that affect through-bond energy-transfer and electron-transfer processes. The results demonstrate that it is possible to design and prepare synthetic, porphyrin-based antenna−reaction center complexes that mimic the basic photochemical functions of natural photosynthetic light-harvesting antennas and reaction centers in simple, structurally well-defined constructs.

Introduction

The defining event of photosynthesis is the conversion of energy from sunlight to electrochemical potential energy via photoinduced electron transfer in the reaction center. However, this pigment−protein complex does not, in general, absorb the actinic light directly. Rather, an antenna array gathers sunlight and donates the resulting excitation energy to the reaction center chlorophylls via singlet−singlet energy transfer. Mimicry of the photosynthetic process by artificial systems holds promise for technological advances in solar energy conversion, molecule-based optoelectronics, and a variety of other applications. Many of the initial investigations of artificial photosynthesis naturally focused on the photoinduced electron-transfer processes, and many reaction center mimics have been prepared and studied. A large class of such mimics is based on porphyrins or related chromophores covalently linked to electron donor or acceptor moieties, or both. Some of these molecules demonstrate quantum yields, efficiencies, and lifetimes for charge separation that are comparable to those found in natural reaction centers.[1−10]

Mimicry of antenna function has also been investigated. Singlet energy transfer between two, or a few, linked porphyrins or other chromophores has been studied extensively. More recently, covalently linked and self-assembled multiporphyrin arrays have been constructed and, in some cases, shown to exhibit singlet−singlet energy transfer between chromophores.[11−39] Some of these constructs have potential as photonic "wires" and switches.[40,41]

The progress in artificial systems in these two areas suggests the possibility of combining an artificial light-harvesting array with a reaction center mimic to produce a complex capable of absorbing light, transferring the resulting excitation to an energy sink, and using the captured energy to initiate photoinduced electron transfer. We recently reported the synthesis and spectroscopic investigation of antenna−reaction center mimic **1**, which consists of four covalently linked zinc tetraarylporphyrins, $(P_{ZP})_3-P_{ZC}$, joined to a free-base porphyrin−fullerene artificial photosynthetic reaction center, $P-C_{60}$, to form a $(P_{ZP})_3-P_{ZC}$-$P-C_{60}$ hexad (Chart 1).[42] The molecule was studied in 2-methyltetrahydrofuran solution using time-resolved absorption and emission techniques. In this array, excitation of any peripheral zinc porphyrin moiety (P_{ZP}) is followed by singlet−singlet energy transfer to the central zinc porphyrin to give

† Part of the special issue "Noboru Mataga Festschrift".
* To whom correspondence should be addressed.
[#] Arizona State University.
[§] North Carolina State University.

10.1021/jp012133s CCC: $22.00
Published on Web 02/06/2002

CHART 1

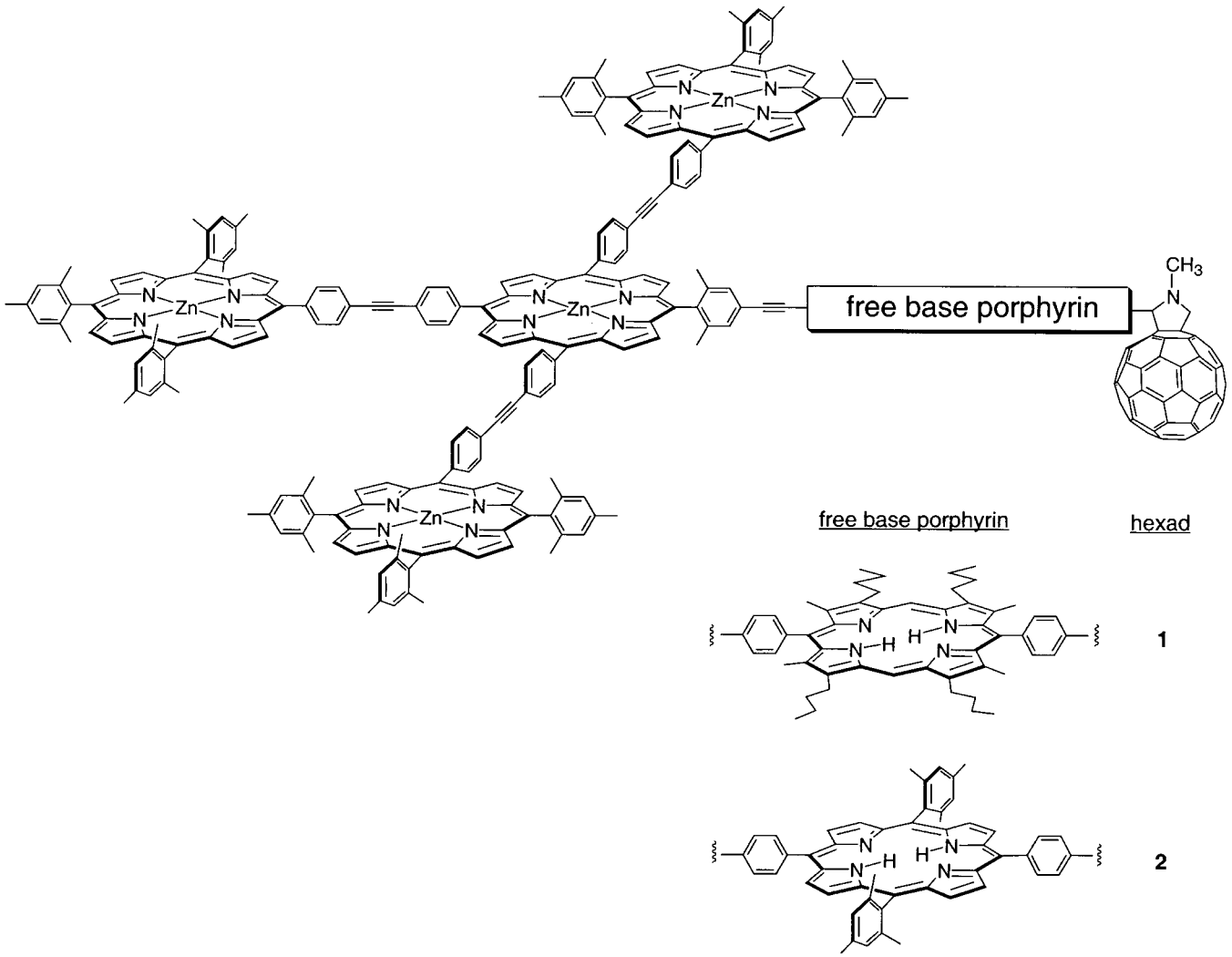

$(P_{ZP})_3-{}^1P_{ZC}-P-C_{60}$ with a time constant of 50 ps. The excitation is passed on to the free-base porphyrin in 240 ps to produce $(P_{ZP})_3-P_{ZC}-{}^1P-C_{60}$, which decays by electron transfer to the fullerene with a time constant of 3 ps. The $(P_{ZP})_3-P_{ZC}-P^{\bullet+}-C_{60}^{\bullet-}$ charge-separated state thus formed has a lifetime of 1.3 ns and is generated with a quantum yield of 0.70 based on light absorbed by the zinc porphyrin antenna.

Although this molecular hexad demonstrated the feasibility of preparing an artificial antenna−reaction center complex, its overall performance left room for improvement. The quantum yield of charge separation is not unity, as it is in photosynthesis, mainly because of slow and therefore inefficient singlet−singlet energy transfer from the central zinc porphyrin of $(P_{ZP})_3-{}^1P_{ZC}-P-C_{60}$ to the free-base porphyrin, from which photoinduced electron transfer occurs. In addition, the lifetime of the $(P_{ZP})_3-P_{ZC}-P^{\bullet+}-C_{60}^{\bullet-}$ charge-separated state is short because of relatively strong electronic coupling between the free-base porphyrin and the fullerene. In our report,[42] we suggested some possible "molecular engineering" that was expected to improve the performance of the hexad. For example, the rate constant for and yield of singlet−singlet energy transfer should be increased by optimal selection of the porphyrin frontier molecular orbitals and steric factors for enhanced through-bond energy transfer. Tuning of redox potentials or addition of new donor and acceptor moieties or both would allow additional decoupling of the radical ions thereby creating longer-lived charge-separated states.

With these considerations in mind, we designed hexad **2** (Chart 1), in which the free-base diaryloctaalkylporphyrin of **1** has been replaced by a *meso*-tetraarylporphyrin. This change was expected to accomplish two important things. First, as has been previously noted,[15,42−44] singlet−singlet energy transfer via linkers attached to the meso positions of the porphyrin is expected to be faster for tetraarylporphyrins such as the free-base porphyrin of **2** than for octaalkylporphyrins such as the free-base porphyrin in **1**. Accordingly, replacement of the β-substituted porphyrin by the meso-substituted porphyrin should increase the singlet−singlet energy-transfer rate from the central zinc porphyrin to the free-base porphyrin and therefore increase the yield of charge separation. The reasons for this will be discussed below. Second, the tetraarylporphyrin employed in **2** is expected to have a higher oxidation potential than does the octaalkylporphyrin analogue in **1**. This is expected to increase the thermodynamic driving force for the charge shift reaction of $(P_{ZP})_3-P_{ZC}-P^{\bullet+}-C_{60}^{\bullet-}$ to yield $(P_{ZP})_3-P_{ZC}^{\bullet+}-P-C_{60}^{\bullet-}$. The latter state might undergo further hole transfer to yield $P_{ZP}^{\bullet+}-(P_{ZP})_2-P_{ZC}-P-C_{60}^{\bullet-}$. These states feature less electronic coupling between the radical ions than does $(P_{ZP})_3-P_{ZC}-P^{\bullet+}-C_{60}^{\bullet-}$ and would be expected to have longer lifetimes. As detailed below, hexad **2** lives up to these expectations.

Results

Synthesis. The starting point for the synthesis of hexad **2** is the previously reported zinc porphyrin tetrad **3** (Chart 2).[42,45]

CHART 2

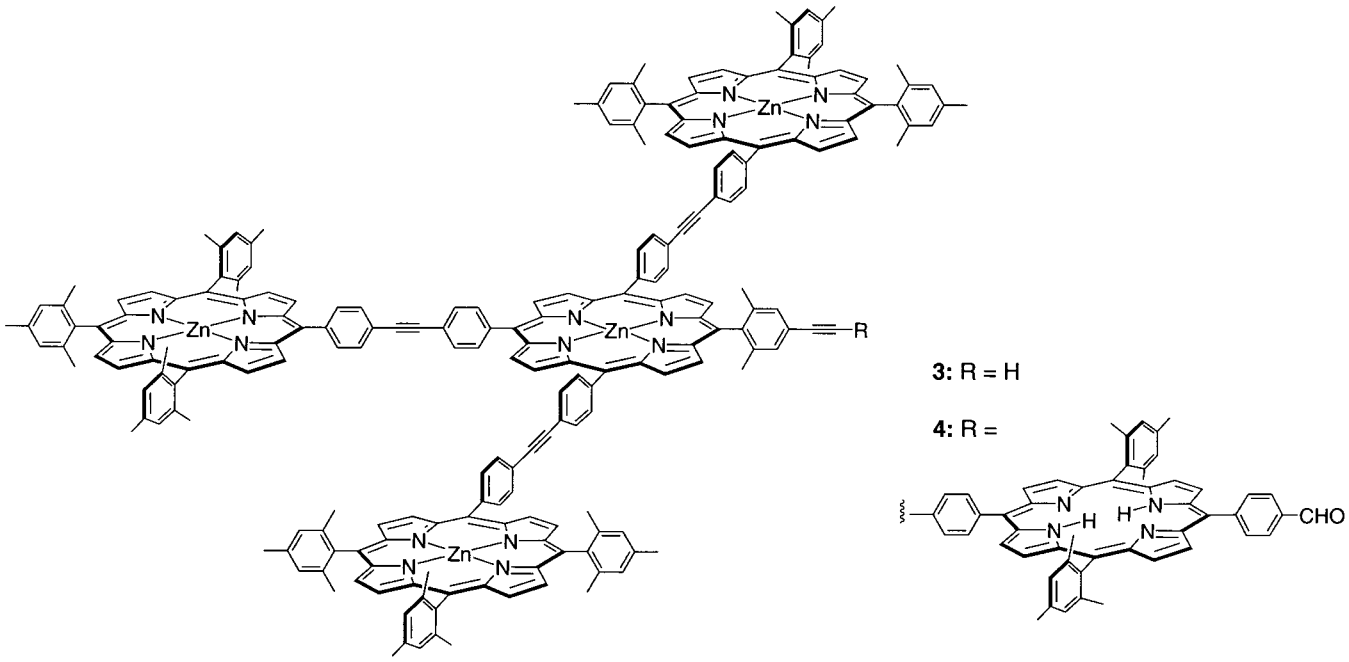

Palladium-induced coupling of **3** with 5-(4-formylphenyl)-15-(4-iodophenyl)-10,20-dimesitylporphyrin yielded pentad **4** (Chart 2), a free-base porphyrin bearing both the zinc antenna module and an aldehyde. Reaction[46] of **4**, C_{60}, and sarcosine gave **2** in 71% yield. Such reactions are known to produce only a single isomer: an adduct to a double bond at a 6,6-ring fusion in C_{60}. Hexad **2** was characterized by NMR spectroscopy and mass spectrometry. The various model compounds used in this study were prepared by similar methods, and details are given in the Experimental Section. These compounds are soluble in the organic solvents employed to a greater extent than is necessary for the various spectroscopic studies described below, and aggregation in solution was not observed.

Cyclic Voltammetry. Cyclic voltammetric measurements were performed to estimate the energies of the various charge-separated states that could be formed from **2** as a result of photoinduced electron transfer. The P−C_{60} dyad **5** in benzo-

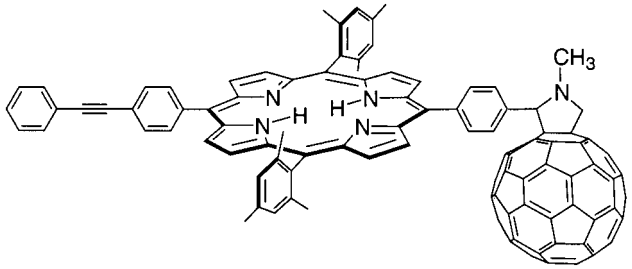

5

nitrile solution containing 0.1 M tetra-*n*-butylammonium hexafluorophosphate and ferrocene as an internal redox standard was found to exhibit a first oxidation potential of 0.64 V (1.05 V vs SCE), which is ascribed to the free-base porphyrin moiety on the basis of results for model porphyrins. The first reduction potential of −1.03 V (−0.62 V vs SCE) is due to formation of the fullerene radical anion.

The cyclic voltammogram of zinc porphyrin antenna **3** showed a broad first oxidation wave at a potential of ∼0.36 V (0.77 V vs SCE). This wave is ascribed to oxidation of the central and peripheral zinc porphyrin moieties, the potentials of which evidently differ only slightly. A single first reduction potential of −1.85 V (−1.43 V vs SCE) was measured.

Absorption Spectra. The absorption spectrum of a 2-methyltetrahydrofuran solution of hexad **2** in the Q-band region is shown in Figure 1. Porphyrin absorption maxima are observed at 649, 598, 558, 515, 486(sh), 433, and 425 nm. In addition, the longest-wavelength maximum of the fullerene is found at 705 nm (see inset). The zinc porphyrin Soret bands are excitonically split, as previously noted for similar zinc porphyrin arrays and **1**.[42] The excitonic splitting for **2** is 7.5 nm, and the oscillator strength is larger for the longer-wavelength transition. For comparison, spectra of model pentad **4** and P−C_{60} dyad **5**, normalized at the 649 nm band, are also shown. Absorption maxima for model dyad **5** occur at 649, 592, 549, 515, 483, and 419 nm.

Linear analysis of the absorption spectrum of **2** in terms of appropriate models, shown in Figure 1, indicates that although electronic interactions between the zinc porphyrins lead to perturbation of the Soret bands, the long-wavelength (Q-band) absorptions of all porphyrins and the fullerene are negligibly affected when the pigments are linked to form the array. In the point-dipole approximation, exciton theory indicates that the

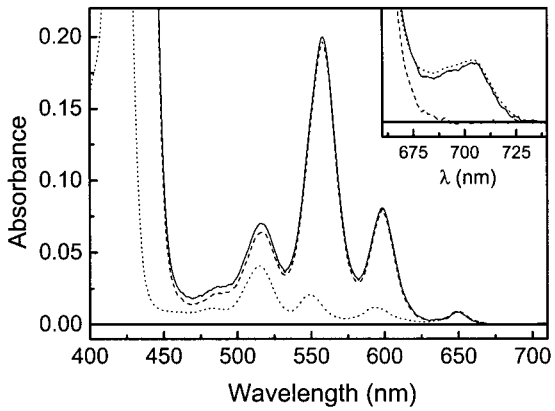

Figure 1. Absorption spectra in 2-methyltetrahydrofuran of hexad **2** (—), model porphyrin array **4** (− − −), and model dyad **5** (···). The inset is an expansion of the fullerene long-wavelength absorption region.

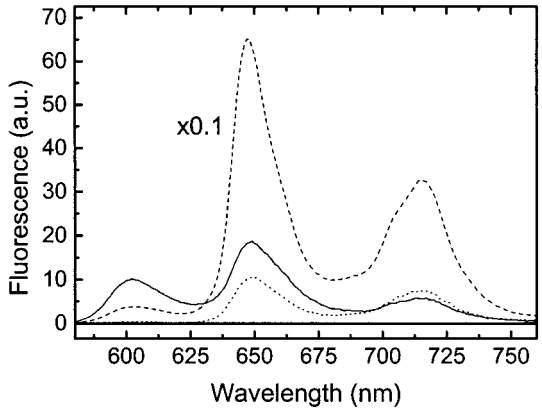

Figure 2. Fluorescence emission spectra in 2-methyltetrahydrofuran solution of hexad **2** (—), model porphyrin array **4** (– – –), and model dyad **5** (···) with excitation at 560 nm, where the zinc porphyrin moiety absorbs a large fraction of the light. All samples had the same optical density at 560 nm. The fluorescence intensity of **4** has been reduced by a factor of 10 for ease in visualization.

interaction between chromophores should be inversely proportional to the cube of the interchromophoric distance and proportional to the square of the transition moments of the interacting chromophores. Thus, long-range exciton coupling in the zinc porphyrin arrays should only be seen for the high-oscillator-strength Soret bands and not for the weaker Q-bands, as is observed.[47,48]

The analysis indicates that in the Soret region (not shown) the free-base porphyrin contributes only a small shoulder around 419 nm and most of the absorption is due to the zinc porphyrins. Significant selectivity in excitation of the zinc porphyrin antenna may also be achieved at 560 nm, at which these moieties dominate the spectrum. It is possible to selectively excite the free-base porphyrin at 650 nm or the fullerene at 705 nm without absorption by the zinc antenna.

Fluorescence Emission. The fluorescence emission spectra of **2**, **4**, and **5** in 2-methyltetrahydrofuran are shown in Figure 2. The samples had the same absorbance at the excitation wavelength of 560 nm. In hexad **2** and pentad **4**, most of the excitation light is absorbed by the zinc porphyrin moieties. The emission spectrum of dyad **5** is typical of that of a free-base porphyrin with maxima at 649 and 714 nm. The emission spectra of **2** and **4** show similar emission from the free-base porphyrin and, in addition, feature maxima for the zinc porphyrins at 602 and 649 nm. Quantitative comparisons show that the emission of the free-base porphyrin moiety in **2** and **5** is reduced by a factor of ~50, relative to that of **4**, which lacks the fullerene moiety. This suggests that the first excited singlet state of the free-base porphyrin moiety of **2** and **5** is strongly quenched by the attached fullerene. Comparison of the zinc porphyrin fluorescence intensity in pentad **4** at 602 nm with that of the free-base porphyrin emission at 714 nm indicates that zinc porphyrin fluorescence is also strongly quenched. As discussed in detail below, this is due to singlet−singlet energy transfer from the zinc porphyrin antenna to the free-base porphyrin.

Time-Resolved Fluorescence. To learn more about the nature of the fluorescence quenching, time-resolved fluorescence experiments were undertaken using the single-photon-timing technique (Figure 3).

Pentad 4. Experiments were carried out with model pentad **4**, which lacks the fullerene. The sample in 2-methyltetrahydrofuran was excited at 560 nm (absorption mainly by the zinc porphyrins), and kinetics were measured at eight wavelengths in the 600−750 nm region. Global analysis of the data

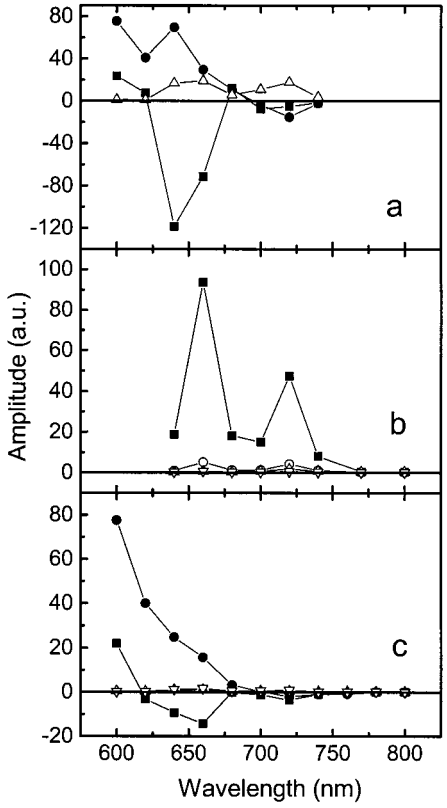

Figure 3. Decay-associated fluorescence spectra of **4**, **5**, and **2** in 2-methyltetrahydrofuran solution with excitation at 560 nm: (a) porphyrin pentad **4** at (■) 9 ps, (●) 160 ps, (△) and 11 ns, $\chi^2 = 1.11$; (b) free-base P−C_{60} dyad **5** at (■) 25 ps, (○) 200 ps, (△) 2 ns, (▽) 10 ns, $\chi^2 = 1.12$; (c) hexad **2** at (■) 9.5 ps, (●) 160 ps, (△) 855 ps, (▽) 10 ns, $\chi^2 = 1.18$.

as three exponential components ($\chi^2 = 1.11$) yielded lifetimes of 9.0 ps, 160 ps, and 11.0 ns. The results are shown in Figure 3a. The spectrum of the 9.0 ps component shows a positive amplitude at 600 nm, at which the zinc porphyrin first excited singlet states emit, a strong negative amplitude around 650 nm, at which both types of porphyrin moieties emit, and a small negative amplitude in the 720 nm region due to emission from the free-base porphyrin (Figure 2). The 160 ps component has a positive amplitude in the 600 nm region, but a negative amplitude for free-base porphyrin emission around 720 nm. Negative amplitudes denote an increase in fluorescence intensity with time after the laser pulse is over, which is indicative of singlet−singlet energy transfer. The significant shortening of the lifetimes of the zinc porphyrin first excited singlet states relative to the 2.4 ns lifetime of the corresponding states in typical zinc porphyrins of this type[42] is also consistent with singlet−singlet energy transfer to the free-base porphyrin, as are the steady-state emission spectra discussed above. Thus, these decay-associated spectra are indicative of singlet−singlet energy transfer among the four zinc porphyrin moieties in the antenna and to the free-base porphyrin to form $(P_{ZP})_3-P_{ZC}-{}^1P$. As described later, the various zinc porphyrin excited states are of similar energy and in equilibrium with one another, and both of the picosecond decay components feature characteristics of both energy-transfer processes.

The 11 ns component of the decay has the emission spectrum of a free-base porphyrin and thus represents the decay of $(P_{ZP})_3-P_{ZC}-{}^1P$. This lifetime is typical for an unperturbed free-base porphyrin of this type and indicates that $(P_{ZP})_3-P_{ZC}-{}^1P$ is not significantly quenched by either electron transfer involving the

zinc porphyrin moieties or back transfer of singlet excitation energy to the zinc porphyrins.

Dyad 5. Time-resolved fluorescence experiments were also carried out with P−C_{60} dyad **5** (Figure 3b). The sample in 2-methyltetrahydrofuran was excited at 560 nm, and kinetics were measured at eight wavelengths in the 600−800 nm region. Global analysis of these data ($\chi^2 = 1.11$) yielded one significant decay component with a lifetime of 25 ps. Additional minor components (≤5% of the decay) were also required to fit the data; these are ascribed to minor impurities or fitting artifacts. The spectrum of the 25 ps decay component is similar to that of a free-base porphyrin with maxima at ∼650 and ∼720 nm. The significant shortening of the lifetime of this state relative to those of the corresponding states in typical free-base porphyrins of this type (e.g., the 11 ns lifetime observed for the free-base porphyrin in **4**) is ascribed to photoinduced electron transfer to the fullerene (vide infra). We do not observe any corresponding rise of fluorescence from the fullerene moiety in the 800-nm region, suggesting that singlet energy transfer from the porphyrin to the fullerene is not a major decay pathway. However, because fullerene excited states in similar molecules are strongly quenched by electron transfer from the adjacent porphyrin, observation of such transfer can be difficult. A small amount of singlet energy transfer from porphyrin to an attached fullerene has been observed in a related porphyrin−fullerene dyad.[49]

Hexad 2. Fluorescence emission from a 2-methyltetrahydrofuran solution of hexad **2** was also studied by the single-photon-timing technique. Excitation was at 560 nm, and the fluorescence was measured at 11 wavelengths in the 600−800 nm region. Global analysis of these data ($\chi^2 = 1.18$) yielded two significant decay components with lifetimes of 9.5 and 160 ps (Figure 3c). Two additional components (≤5% of the decay) were also required to fit the data and are ascribed to minor impurities or fitting artifacts. Both major components are similar to the two picosecond components observed in pentad **4** and indicate singlet−singlet energy transfer among the zinc porphyrin moieties and ultimately to the free-base porphyrin to give $(P_{ZP})_3-P_{ZC}-{}^1P-C_{60}$.

No significant emission from the free-base porphyrin of **2** was detected in the time-resolved experiments. The lack of emission from the free-base porphyrin is ascribed to rapid quenching of $(P_{ZP})_3-P_{ZC}-{}^1P-C_{60}$ due to photoinduced electron transfer to the fullerene to yield $(P_{ZP})_3-P_{ZC}-P^{\bullet+}-C_{60}^{\bullet-}$ and to the fact that excitation was at 560 nm at which most of the absorption, and consequent emission, is due to the zinc porphyrin antenna. These results are consistent with the steady-state measurements, in which only very weak emission from the free-base porphyrin (due possibly to a minor impurity) was detected.

Transient Absorption with 100 fs Excitation. Transient absorption experiments were undertaken to better quantify the interconversions of the various excited states in these compounds and to allow detection of nonemissive states such as charge-separated species. Solutions of **2**, **4**, and **5** in 2-methyltetrahydrofuran (∼1×10^{-3} M) were excited with ∼100 fs laser pulses, and the transient absorption was recorded using the pump−probe method. Transient spectra were recorded in the 450−760 nm and 930−1070 nm regions. A total of 155 and 70 kinetic traces, respectively, were measured, at times ranging from −50 to 4500 ps relative to the laser flash. Data were fitted globally using singular-value decomposition methods.[50,51] Random error was typically ≤5%.

Dyad 5. Verification of the formation of $P^{\bullet+}-C_{60}^{\bullet-}$ by photoinduced electron transfer comes from a spectroscopic investigation of porphyrin−fullerene dyad **5**. The inset in Figure 4 shows the transient absorption spectrum in the 930−1070 nm region 500 ps after excitation of the sample at 650 nm, at which most of the absorption is due to the porphyrin moiety. The band centered at ∼1000 nm is due to the fullerene radical anion of the $P^{\bullet+}-C_{60}^{\bullet-}$ charge-separated state.[52] Also shown in Figure 4 is the rise of the transient absorption at 1000 nm following excitation. A small prompt absorption due mainly to the porphyrin excited singlet state ${}^1P-C_{60}$ is followed by the grow-in of the absorption maximum. This rise was fitted as a single exponential with a time constant of 25 ps. Thus, ${}^1P-C_{60}$ decays in 25 ps by photoinduced electron transfer to yield $P^{\bullet+}-C_{60}^{\bullet-}$. Also shown is the decay of the charge-separated state, which occurs with a time constant of 3.0 ns.

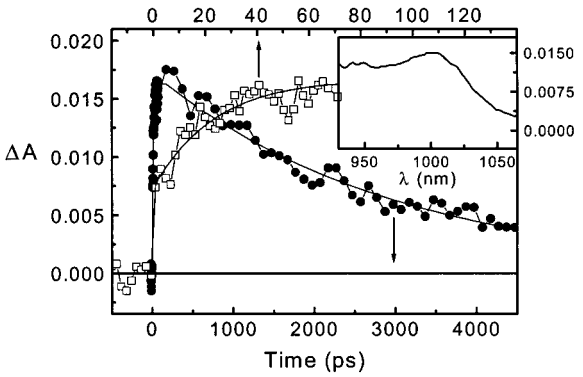

Figure 4. Transient absorption kinetics measured for 2-methyltetrahydrofuran solutions of dyad **5** with excitation at 650 nm: (□) rise of the transient absorption at 1000 nm and exponential fitting with a time constant of 25 ps (upper axis); (●) decay of the transient at 1000 nm and exponential fitting with a time constant of 3.0 ns (lower axis). The inset shows the transient absorption spectrum measured 500 ps after excitation.

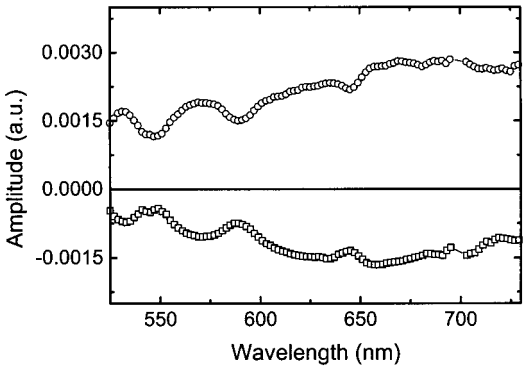

Figure 5. Decay-associated spectra for dyad **5** in 2-methyltetrahydrofuran obtained from a global analysis of the transient absorption data taken after excitation of the fullerene moiety at 705 nm. The lifetimes of the components are 75 ps (□) and 3.0 ns (○). In these decay-associated spectra, a component with a negative amplitude represents a transient that *increases* in intensity with time following excitation.

Figure 5 shows decay-associated spectra obtained by a global analysis of the data for dyad **5** with excitation at 705 nm, at which only the fullerene absorbs light. A component with a lifetime of 75 ps having negative amplitude throughout the region was observed. The negative amplitude signifies a transient the absorption of which is increasing (growing in) during the time period of observation. The spectrum is characteristic of the porphyrin radical cation absorption, which features bleaching of the ∼550, ∼590, and ∼650 nm bands associated with ground-state absorption (Figure 2) superimposed upon a broad, relatively featureless absorption band. The 75 ps component is assigned to formation of $P^{\bullet+}-C_{60}^{\bullet-}$ from the fullerene first excited singlet

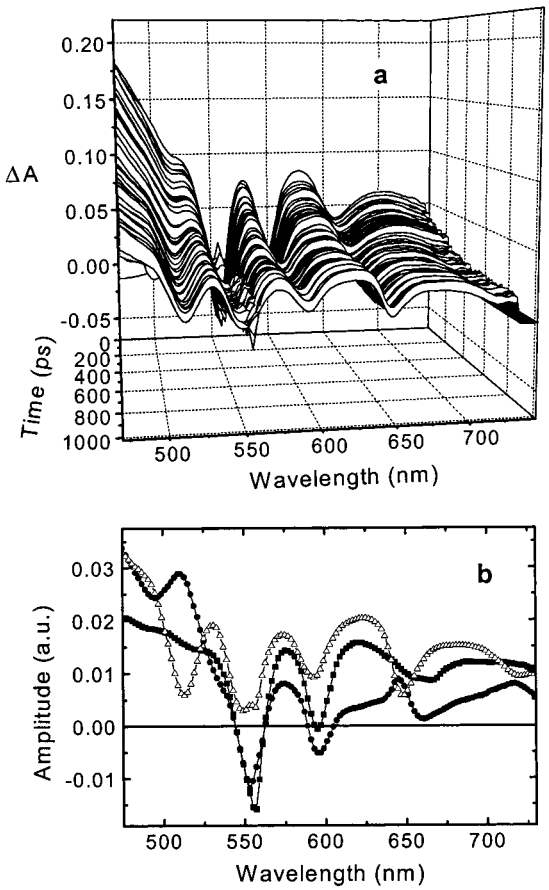

Figure 6. Typical transient absorption data (a) for pentad **4** in 2-methyltetrahydrofuran taken after excitation at 560 nm and decay-associated spectra (b) for pentad **4** obtained from a global analysis of the data set in panel a. The lifetimes of the components are 9.5 ps (■), 160 ps (●), and 11.0 ns (△).

state, $P-{}^1C_{60}$, by photoinduced electron transfer. A second component with a time constant of 3.0 ns has a positive amplitude, which indicates a decay with time after the laser pulse. Its shape is the mirror image of the 75 ps component, suggesting that it is due to the same chemical species. Thus, we assign the 3.0 ns time constant to the decay of $P^{\bullet+}-C_{60}^{\bullet-}$ to the ground state. The significantly smaller time constant for formation of the charge-separated state from $^1P-C_{60}$ relative to that for formation of this state from $P-{}^1C_{60}$ (25 vs 75 ps) verifies that $^1P-C_{60}$ decays mainly by direct electron transfer to the fullerene, rather than energy transfer to the fullerene followed by photoinduced electron transfer.

Pentad 4. Verification of the singlet−singlet energy transfer from the chromophores of the zinc porphyrin antenna to the free-base porphyrin comes from the transient absorption results for pentad **4** (Figure 6). Samples were excited at 560 nm, at which most of the absorption is due to the zinc porphyrin. Figure 6b shows the decay-associated spectra obtained by a global analysis of the data. Consistent with the time-resolved fluorescence measurements (Figure 3), there are three components with lifetimes of 9.5 ps, 160 ps, and 11.0 ns. The two picosecond components show spectra characteristic of the zinc porphyrin first excited singlet state, with bleaching bands at 550 and 600 nm and stimulated emission at 650 nm. The 160 ps component spectrum also has maxima at wavelengths characteristic of bleaching of the free-base porphyrin bands at 515 and 650 nm and stimulated emission from the free-base porphyrin at 720 nm. These features indicate formation of $(P_{ZP})_3-P_{ZC}-{}^1P$ associated with the 160 ps lifetime.

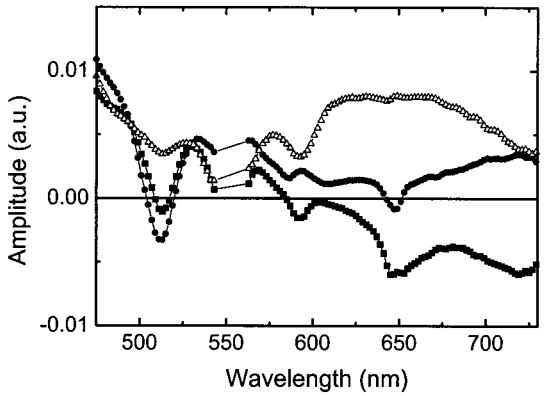

Figure 7. Decay-associated spectra for hexad **2** in 2-methyltetrahydrofuran obtained from a global analysis of transient absorption data taken after excitation at 650 nm, at which most of the excitation is to the free-base porphyrin. The lifetimes of the components are 25 ps (■), 380 ps (●), and fixed at 240 ns (nondecaying on this time scale) (△).

The 11 ns component in Figure 6 has a spectrum characteristic of the free-base porphyrin, with bleaching bands at 515, 550, 590, and 650 nm and stimulated emission at 720 nm. This represents the decay of $(P_{ZP})_3-P_{ZC}-{}^1P$. Taken together, the data for **4** are consistent with singlet−singlet energy transfer among the zinc porphyrins in the antenna array and ultimately to the free-base porphyrin.

Hexad 2. Figure 7 shows the decay-associated spectra for hexad **2** obtained by a global analysis of data obtained with excitation at 650 nm at which the free-base porphyrin absorbs and the zinc porphyrins do not. The best fit was achieved with three components, one of which was nondecaying on this time scale. The 25 ps component is mostly of negative amplitude and has bands at 515, 550, 590, 650, and 720 nm, which are characteristic of the free-base porphyrin and can be assigned to formation of the radical cation. These results reflect the formation of the $(P_{ZP})_3-P_{ZC}-P^{\bullet+}-C_{60}^{\bullet-}$ charge-separated state from $(P_{ZP})_3-P_{ZC}-{}^1P\ -C_{60}$ with the same time constant as observed for model dyad **5** (Figure 3). The 380 ps component is mostly of positive amplitude and has almost the same bleaching bands as the 25 ps component. It should be noted that this component has negative amplitude at the maxima of the 515 and 650 nm bleaching bands, which are characteristic only of the free-base porphyrin. The negative amplitude in this case indicates a rise of a transient species that does not have bleaching bands at those wavelengths. This species is seen as well in the fixed component, which is characteristic of the zinc porphyrin radical cation with bleaching only at 550 and 600 nm. Taken together, these data show the formation of $(P_{ZP})_3-P_{ZC}-P^{\bullet+}-C_{60}^{\bullet-}$ from $(P_{ZP})_3-P_{ZC}-{}^1P-C_{60}$ with a time constant of 25 ps, and the 380 ps decay of $(P_{ZP})_3-P_{ZC}-P^{\bullet+}-C_{60}^{\bullet-}$ by electron transfer from the zinc porphyrin system to yield a final $((P_{ZP})_3-P_{ZC})^{\bullet+}-P-C_{60}^{\bullet-}$ charge-separated state that does not decay on the time scale of the measurement.

Transient Absorption with 5 ns Excitation. To determine the ultimate fate of the charge-separated state formed by excitation of hexad **2**, deoxygenated samples of the compound in 2-methyltetrahydrofuran were excited with ∼5 ns laser pulses at 560 nm and the resulting transient species were detected. Figure 8 shows the resulting kinetic traces. One of these, featuring a decay time of 240 ns, was determined at 1000 nm and reports on the decay of the fullerene radical anion absorption. The second, measured at 570 nm, reflects the recovery of the ground-state bleach due to the zinc porphyrin radical cation (see Figure 7) and was also fitted as an exponential

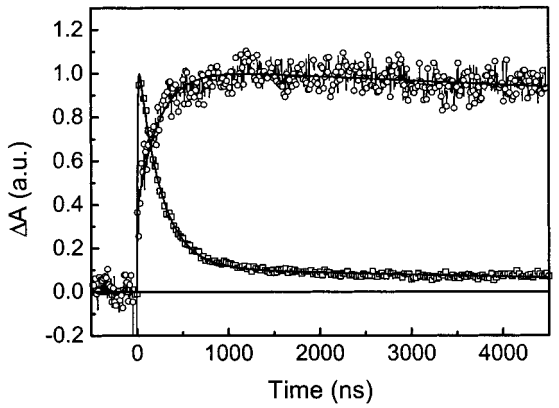

Figure 8. Transient absorption kinetics measured for hexad **2** in 2-methyltetrahydrofuran at 1000 nm (□) and 570 nm (○) following excitation at 560 nm at which most of the absorption is due to the zinc porphyrin antenna system. Two-exponential fits to the data with time constants of 240 ns (major) and 140 μs (minor) are shown as smooth curves.

process with a time constant of 240 ns. Thus, $((P_{ZP})_3-P_{ZC})^{\bullet+}-P-C_{60}^{\bullet-}$ decays with a lifetime of 240 ns.

The decays in Figure 8 both required two exponential components for a satisfactory fit. The long, minor component apparent in the figure has a lifetime of tens of microseconds at both wavelengths. The lifetime of this, and only this, component was shortened in the presence of oxygen, and it is attributed to the triplet states of **2**. Spectra taken at various times confirm this interpretation. At early times, the fullerene radical anion absorption at ~1000 nm is observed, but at later times, only the porphyrin triplet absorption around 780 nm is seen. The charge recombination of $((P_{ZP})_3-P_{ZC})^{\bullet+}-P-C_{60}^{\bullet-}$ is not accompanied by the formation of significant amounts of triplet states and is dominated by recovery of the singlet ground state.

In benzonitrile solution, the $((P_{ZP})_3-P_{ZC})^{\bullet+}-P-C_{60}^{\bullet-}$ charge-separated state decays with a lifetime of 25 μs. This long lifetime provides the opportunity for significant reaction with molecular oxygen. Admission of air to the benzonitrile solution of **2** resulted in a markedly accelerated decay of the fullerene radical anion absorption. This leads to the thermodynamically supportable conclusion that $C_{60}^{\bullet-}$ is oxidized by oxygen, as has been observed in a fullerene-based triad molecule.[52]

Discussion

Kinetic Components. Although the photochemistry of multichromophoric **2** is necessarily complex, the combination of time-resolved fluorescence and absorption experiments has allowed extraction of several lifetimes for kinetic processes. The time-resolved fluorescence data (Figure 3) yield time constants of 9.5 and 160 ps that are associated with the zinc porphyrin moieties. The shortening of the zinc porphyrin singlet lifetime from 2.4 ns in previously reported tetrad[42] **3** to give 9.5 and 160 ps components in **4** and **2** is a result of singlet−singlet energy transfer from the zinc porphyrins to the free-base porphyrin. In addition, fluorescence from the free-base porphyrin of **2** is very strongly quenched from its usual lifetime of 11 ns, and the transient absorbance results yield additional time constants of 25 ps, 380 ps, and 240 ns. These values can be related to physically significant processes in the hexad by use of a suitable kinetic model.

Analysis of Kinetic Data. The model chosen for interpretation of the kinetic and spectroscopic data dealing with singlet energy transfer and electron transfer in hexad **2** is shown in Figure 9. The energies of the various spectroscopic states were

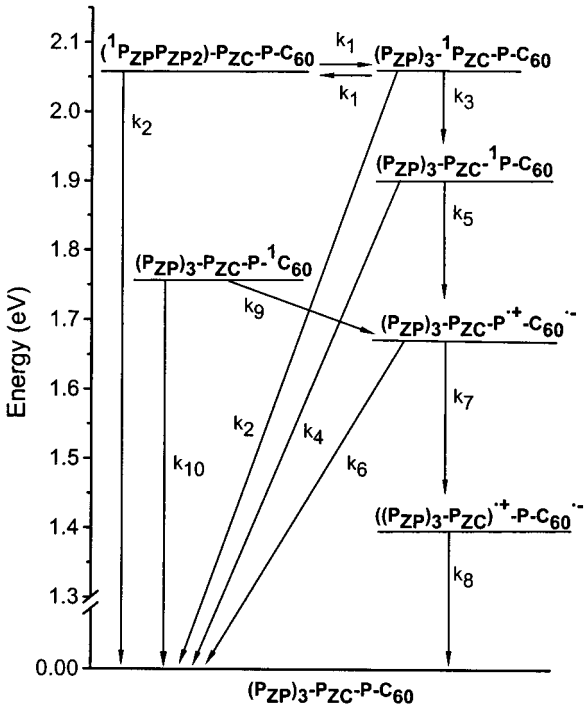

Figure 9. Transient states of hexad **2** and relevant interconversion pathways. The energies of the various states have been estimated as discussed in the text, and no correction for possible Coulombic effects on the energies of the charge-separated states has been made.

determined from the wavelength average of the longest-wavelength absorption and shortest-wavelength emission maxima of **2** and appropriate model compounds. The zinc porphyrin first excited singlet states lie at 2.06 eV, $(P_{ZP})_3-P_{ZC}-^1P-C_{60}$ is 1.91 eV above the ground state, and the fullerene first excited singlet state is at 1.75 eV. The energies of the $(P_{ZP})_3-P_{ZC}-P^{\bullet+}-C_{60}^{\bullet-}$ and $((P_{ZP})_3-P_{ZC})^{\bullet+}-P-C_{60}^{\bullet-}$ charge-separated states were estimated as 1.67 and ~1.39 eV, respectively, on the basis of the electrochemically determined oxidation potentials of the porphyrins and reduction potential of the fullerene in model tetrad **3** and dyad **5** discussed above. The triplet states $(P_{ZP})_3-P_{ZC}-^3P-C_{60}$ and $(P_{ZP})_3-P_{ZC}-P-^3C_{60}$ lie at approximately 1.4 and 1.5 eV, respectively, whereas the zinc porphyrin triplet state is at ~1.53 eV.[53,54]

The following assumptions and conclusions, which are supported by the spectroscopic results discussed in the previous section, were made in the analysis of **2**:

(a) The four zinc porphyrin moieties of **2** are essentially isoenergetic and equivalent in their inherent excited-state properties. The rate constants for singlet−singlet energy transfer among all four of these porphyrins are equal, with a value k_1. These assumptions are supported by the results of previous spectroscopic studies of closely related multiporphyrin arrays[12] and hexad **1**.

(b) The rate constants for decay of each of the zinc porphyrin first excited singlet states by the usual photophysical pathways of fluorescence, intersystem crossing, and internal conversion are identical with $k_2 = 4.2 \times 10^8$ s^{-1} on the basis of the 2.4 ns lifetime determined for model compound **3**.

(c) Singlet−singlet energy transfer from $(P_{ZP})_3-^1P_{ZC}-P-C_{60}$ to the free-base porphyrin, giving $(P_{ZP})_3-P_{ZC}-^1P-C_{60}$, occurs with a rate constant k_3. It is assumed that there is no back energy transfer from the free-base porphyrin to the zinc porphyrin antenna array, given the fluorescence results for model compound **4** and the fact that such a process is endergonic. It is also assumed that the peripheral zinc porphyrin moieties

transfer excitation only to the central zinc porphyrin and not directly to the free-base porphyrin or directly to each other. Electronic communication among nonadjacent sites is known to occur, albeit at slower rates, and has been neglected in this pairwise model.[55]

(d) The rate constant k_4 for decay of the free-base porphyrin first excited singlet state $(P_{ZP})_3-P_{ZC}-{}^1P-C_{60}$ by the usual photophysical pathways is 1×10^8 s^{-1} on the basis of the 11 ns lifetime determined for model compound **4**.

(e) The $(P_{ZP})_3-P_{ZC}-{}^1P-C_{60}$ excited state is quenched only by electron transfer to the fullerene moiety with a rate constant k_5. As mentioned above, energy transfer to the fullerene followed by photoinduced electron transfer is negligible in **2**.

(f) Charge recombination of $(P_{ZP})_3-P_{ZC}-P^{\bullet+}-C_{60}^{\bullet-}$ occurs to yield the ground state with a rate constant k_6, as was observed for dyad **5**.

(g) As indicated by the transient absorption results for **2**, electron transfer from the zinc porphyrin array to the free-base porphyrin radical cation in $(P_{ZP})_3-P_{ZC}-P^{\bullet+}-C_{60}^{\bullet-}$ transforms this state into $((P_{ZP})_3-P_{ZC})^{\bullet+}-P-C_{60}^{\bullet-}$ with a rate constant k_7.

(h) As demonstrated by the nanosecond transient absorption results, the final charge recombination process is dominated by recovery of the singlet ground-state with a rate constant k_8 rather than population of a porphyrin triplet excited state.

(i) Multiple excitations of pigments are not considered.

Given these assertions, the singlet energy and electron-transfer processes in **2** are described by the following set of first-order linear differential equations.

$$\frac{d[^1P_{ZP}]}{dt} = -(k_1 + k_2)[^1P_{ZP}] + k_1[^1P_{ZC}] \quad (1)$$

$$\frac{d[^1P_{ZC}]}{dt} = -(3k_1 + k_3 + k_2)[^1P_{ZC}] + 3k_1[^1P_{ZP}] \quad (2)$$

$$\frac{d[^1P]}{dt} = -(k_4 + k_5)[^1P] + k_3[^1P_{ZC}] \quad (3)$$

$$\frac{d[P^{\bullet+}C_{60}^{\bullet-}]}{dt} = -(k_6 + k_7)[P^{\bullet+}C_{60}^{\bullet-}] + k_5[^1P] \quad (4)$$

$$\frac{d[P_Z^{\bullet+}C_{60}^{\bullet-}]}{dt} = -k_8[P_Z^{\bullet+}C_{60}^{\bullet-}] + k_7[P^{\bullet+}C_{60}^{\bullet-}] \quad (5)$$

In these equations, $[^1P_{ZP}]$ represents the concentration of excited states of the peripheral zinc porphyrin moieties, $[^1P_{ZC}]$ is the concentration of excited states of the central zinc porphyrin, $(P_{ZP})_3-{}^1P_{ZC}-P-C_{60}$, $[^1P]$ is the concentration of excited states of the free-base porphyrin, $(P_{ZP})_3-P_{ZC}-{}^1P-C_{60}$, $[P^{\bullet+}C_{60}^{\bullet-}]$ is the concentration of molecules in the charge-separated state $(P_{ZP})_3-P_{ZC}-P^{\bullet+}-C_{60}^{\bullet-}$, and $[P_Z^{\bullet+}C_{60}^{\bullet-}]$ is the concentration of molecules in the charge-separated state $((P_{ZP})_3-P_{ZC})^{\bullet+}-P-C_{60}^{\bullet-}$. It will be noted that although only one equation is written for the three equivalent peripheral zinc porphyrins (eq 1), the absorption of all three must be taken into account when solving the equations numerically.

Solving eqs 1−5 for the concentrations of the relevant species gives the following results.

$$[^1P_Z] = a_1 e^{-\alpha_1 t} + a_2 e^{-\alpha_2 t} \quad (6)$$

$$[^1P] = a_3 e^{-k_4 t} + a_4 e^{-k_5 t} + a_5 e^{-\alpha_1 t} + a_6 e^{-\alpha_2 t} \quad (7)$$

$$[P^{\bullet+}C_{60}^{\bullet-}] = a_7 e^{-k_6 t} + a_8 e^{-k_7 t} + a_9 e^{-k_4 t} + a_{10} e^{-k_5 t} + a_{11} e^{-\alpha_1 t} + a_{12} e^{-\alpha_2 t} \quad (8)$$

$$[P_Z^{\bullet+}C_{60}^{\bullet-}] = a_{13} e^{-k_8 t} + a_{14} e^{-k_6 t} + a_{15} e^{-k_7 t} + a_{16} e^{-k_4 t} + a_{17} e^{-k_5 t} + a_{18} e^{-\alpha_1 t} + a_{19} e^{-\alpha_2 t} \quad (9)$$

$$\alpha_{1,2} = \frac{4k_1 + k_3 + 2k_2}{2} \pm \frac{1}{2}\sqrt{k_3^2 + 4k_1k_3 + 16k_1^2} \quad (10)$$

In these equations, only the total concentration of zinc porphyrin first excited singlet state, $[^1P_Z]$ $(= 3[^1P_{ZP}] + [^1P_{ZC}])$, is given because all four zinc porphyrins are spectroscopically indistinguishable. The α_1 and α_2 values are phenomenological rate constants that would be observed experimentally. The a_i values are amplitudes that depend on the initial conditions (which are determined by the excitation wavelength and extinction coefficients), and only exponential components with significant amplitudes will be observed experimentally.

It will be noted that the rate constants for photoinduced electron transfer (k_5), charge shift (k_7), and charge recombinations (k_6 and k_8) are directly observable experimentally from the results for **2** and model compounds. The photoinduced electron-transfer rate constant (k_5) is determined to be 4.0×10^{10} s^{-1} from the 25 ps time constant detected in the transient absorption experiments on hexad **2** (Figure 7) and the value of (k_4) mentioned previously. This assignment is verified by the results for model $P-C_{60}$ dyad **5**, from which the same value was obtained. The value of rate constant k_6 for charge recombination of $(P_{ZP})_3-P_{ZC}-P^{\bullet+}-C_{60}^{\bullet-}$, 3.3×10^8 s^{-1}, is taken as the reciprocal of the 3.0 ns decay component of the fullerene radical anion absorption observed for dyad **5** (Figure 4). Rate constants k_7 and k_8 equal the reciprocals of the 380 ps (Figure 7) and 240 ns (Figure 8) time constants detected in the transient absorption experiments or 2.6×10^9 and 4.2×10^6 s^{-1}, respectively.

When one has values for the various electron-transfer rate constants, values for the singlet energy-transfer rate constants, k_1 and k_3, are needed. Energy transfer among the various zinc porphyrin moieties is reversible, and the corresponding time constant does not appear directly in the experimental decays, However, it does contribute to the observed values of α_1 and α_2 as per eqs 6−10 and may be extracted using them. Experimentally, α_1 and α_2 can be assigned values of 1.0×10^{11} and 6.3×10^9 s^{-1} from the measured lifetimes of 9.5 and 160 ps. Solving eq 10 using these values and that for k_2 given previously yields values of 2.0×10^{10} s^{-1} for k_1 and 3.1×10^{10} s^{-1} for k_3. The value thus obtained for k_1 is in excellent agreement with the value of 2.0×10^{10} s^{-1} previously reported for hexad **1**.[42] It is also consistent with the work of Hsiao and co-workers,[12] who reported a rate constant of 1.9×10^{10} s^{-1} for singlet energy transfer between two zinc porphyrins in a linear trimeric array with zinc porphyrin substituents and linkages very similar to those in **2**. Thus, despite the complexity of hexad **2**, it is possible to extract all of the relevant rate constants in Figure 9 from the experimental data.

Quantum Yield. The quantum yields of $(P_{ZP})_3-P_{ZC}-P^{\bullet+}-C_{60}^{\bullet-}$ and $((P_{ZP})_3-P_{ZC})^{\bullet+}-P-C_{60}^{\bullet-}$ are, in principle, wavelength-dependent. The quantum yield based on excitation of the zinc porphyrins in the antenna may be determined by simulations of the kinetic pathways in Figure 9 using the rate constants given previously. Simulations were done using IBM's Chemical Kinetics Simulator, version 1.01. The quantum yield of the $(P_{ZP})_3-P_{ZC}-P^{\bullet+}-C_{60}^{\bullet-}$ charge-separated state is thus found to

TABLE 1: Comparison of Hexads 1 and 2

property	hexad **1**	hexad **2**
time constant for P_{ZC} to P energy transfer ($1/k_3$), ps	244	32
time constant for photoinduced electron transfer ($1/k_5$), ps	3	25
lifetime of final charge-separated state, ns	1.3	240
quantum yield[a] of $(P_{ZP})_3-P_{ZC}-P^{\bullet+}-C_{60}^{\bullet-}$	0.70	0.98
quantum yield[a] of $((P_{ZP})_3-P_{ZC})^{\bullet+}-P-C_{60}^{\bullet-}$		0.86
^1P energy, eV	1.96	1.91
P_Z oxidation potential,[b] V	0.77	0.77
P oxidation potential,[b] V	0.84	1.05
energy of $(P_{ZP})_3-P_{ZC}-P^{\bullet+}-C_{60}^{\bullet-}$, eV	1.46	1.67

[a] Based on ^1P_Z. [b] In V vs SCE.

be 0.98, and that of $((P_{ZP})_3-P_{ZC})^{\bullet+}-P-C_{60}^{\bullet-}$ is 0.86. Alternatively, based on the nanosecond transient absorption amplitudes and using the comparative method with *meso*-tetrakis(4-methylphenyl)porphyrin as a standard (porphyrin ϵ_{T-G} at 440 nm = 6.8×10^4 M^{-1} cm^{-1}, $\Phi_T = 0.67$;[56] fullerene radical anion[57] ϵ at 1000 nm = 4700 M^{-1} cm^{-1}), the yield of the $((P_{ZP})_3-P_{ZC})^{\bullet+}-P-C_{60}^{\bullet-}$ charge-separated state in hexad **2** was determined as 0.94, which is in reasonable agreement with the kinetically determined value. The quantum yield of $(P_{ZP})_3-P_{ZC}-P^{\bullet+}-C_{60}^{\bullet-}$ based on direct excitation of the free-base porphyrin is essentially unity, whereas that from excitation of the fullerene moiety ($k_9 = 1.3 \times 10^{10}$ s^{-1}) is 0.95.

Summary of Photochemical Behavior. Although hexad **2** features complex photochemical behavior, the spectroscopic studies described above have allowed elucidation of all of the major energy- and electron-transfer processes and determination of their rate constants. To summarize, light gathered by the peripheral zinc porphyrins in the antenna section of **2** is transferred to the central zinc porphyrin to give $(P_{ZP})_3-{}^1P_{ZC}-P-C_{60}$ with a time constant of 50 ps. In addition to exchanging excitation with the peripheral zinc moieties, this state donates energy to the free-base porphyrin of the artificial reaction center portion with a time constant of 32 ps to yield $(P_{ZP})_3-P_{ZC}-{}^1P-C_{60}$, which decays in 25 ps by photoinduced electron transfer to the fullerene, giving $(P_{ZP})_3-P_{ZC}-P^{\bullet+}-C_{60}^{\bullet-}$. This state is also formed in essentially quantitative yield by photoinduced electron transfer following direct excitation of the free-base porphyrin. Excitation of the fullerene also initiates photoinduced electron transfer to give $(P_{ZP})_3-P_{ZC}-P^{\bullet+}-C_{60}^{\bullet-}$ with a rate constant of 1.3×10^{10} s^{-1}. The $(P_{ZP})_3-P_{ZC}-P^{\bullet+}-C_{60}^{\bullet-}$ state undergoes a charge-shift reaction with a rate constant of 2.3×10^9 s^{-1} to produce the long-lived $((P_{ZP})_3-P_{ZC})^{\bullet+}-P-C_{60}^{\bullet-}$ charge-separated state, which finally decays to the ground state with a lifetime of 240 ns. The first step in this transformation is presumably electron transfer from the central zinc porphyrin to give $(P_{ZP})_3-P^{\bullet+}{}_{ZC}-P-C_{60}^{\bullet-}$. The peripheral and central zinc porphyrin moieties must differ slightly in oxidation potential, and indeed the oxidation wave for **3** in cyclic voltammetry was broad. However, the results do not allow us to decide whether the positive charge remains on the central zinc porphyrin or migrates to the periphery. The quantum yield of $(P_{ZP})_3-P_{ZC}-P^{\bullet+}-C_{60}^{\bullet-}$ is 0.95−0.98, depending upon which chromophore is excited; nearly every absorbed photon leads to charge separation, regardless of its wavelength. The yield of the long-lived $((P_{ZP})_3-P_{ZC})^{\bullet+}-P-C_{60}^{\bullet-}$ state, 0.86, is also high.

Comparison of Two Designs for Integrated Antenna−Reaction Center Complexes. It is interesting to compare the performance of antenna−reaction center complex **2** with the earlier-studied **1**. Selected results for the two molecules in 2-methyltetrahydrofuran are summarized in Table 1. The rate constants for exchange of singlet excitation energy among the zinc porphyrins of the antenna are identical in the two molecules, as one would expect given the structural similarity. On the other hand, the rate constant k_3 for singlet−singlet energy transfer from the central zinc porphyrin of $(P_{ZP})_3-{}^1P_{ZC}-P-C_{60}$ to the free-base porphyrin, yielding $(P_{ZP})_3-P_{ZC}-{}^1P-C_{60}$ is only 4.1×10^9 s^{-1} in **1** but is 3.2×10^{10} s^{-1} in **2**. This factor of 8 leads to an increase in the quantum yield of charge separation from 0.69 in **1** to 0.98 in **2**; the slower rate in **1** allows competition with energy transfer from the usual photophysical pathways that depopulate the zinc porphyrin first excited singlet states.

As mentioned previously, hexad **2** was originally engineered to try to achieve such an increase. Singlet−singlet energy transfer in systems of this type occur mainly by a through-bond mechanism involving orbital overlap rather than the through-space Förster dipole−dipole mechanism.[12,15] In hexad **1**, the free-base porphyrin bears eight alkyl substituents at the β-positions of the pyrrole rings. This substitution pattern destabilizes the a_{1u} orbital, causing the a_{1u} orbital to be the HOMO. The a_{1u} orbital has nodes at the meso positions through which the free-base porphyrin is linked to the zinc porphyrin antenna. The presence of nodes at the meso positions is expected to retard through-bond energy transfer.[15,43,44] The free-base porphyrin in hexad **2**, on the other hand, is of the tetraaryl variety, and features an a_{2u}-type HOMO. The a_{2u} HOMO has lobes at the meso positions, which is expected to facilitate through-bond energy transfer. In addition, through steric effects, the β-substituents of the free-base porphyrin moiety in **1** inhibit rotation of the adjacent aryl rings and lead to an increase in the average dihedral angle between each meso aryl ring and the mean porphyrin plane, relative to that in tetraarylporphyrins such as that in hexad **2**. As the ring approaches orthogonality to the porphyrin, any $\pi-\pi$ overlap contribution to through-bond singlet−singlet energy transfer is reduced.[58,59] Hexad **2** does not suffer from this effect. The overall result is a significant increase in singlet−singlet energy transfer rates for **2**, relative to hexad **1**.

In this connection, it is interesting to note that singlet−singlet energy transfer has also been observed between zinc and free-base tetraarylporphyrins linked by an amide group joining the aryl rings para to the porphyrin macrocycles. Rate constants of 2.3×10^{10} and 1.5×10^{10} s^{-1} were reported for different systems.[52,60,61] Although these systems and **2** differ in porphyrin substitution, solvent conditions, and possibly even the mechanism of singlet−singlet energy transfer, the rate constants for the molecules having the three bonds of the amide linkage and those for the molecules with a three-bond acetylenic linkage are not very different.

Replacement of the free-base octaalkylporphyrin moiety in **1** with the tetraarylporphyrin in **2** was also performed to take advantage of another difference in the properties of the two chromophores. The first oxidation potential for a model for the free-base octaalkylporphyrin moiety of **1** is 0.84 V vs SCE.[42,58] This is not too different from the first oxidation potential of 0.77 V vs SCE found for zinc porphyrins in the antenna moiety. In addition, hole-hopping within diphenylethyne-linked meso-substituted porphyrin arrays is facile.[14,62] This suggests that there is little kinetic and no thermodynamic barrier to transfer of the radical cation in the $(P_{ZP})_3-P_{ZC}-P^{\bullet+}-C_{60}^{\bullet-}$ state of **1** to the zinc porphyrin array to produce $((P_{ZP})_3-P_{ZC})^{\bullet+}-P-C_{60}^{\bullet-}$. However, it also suggests that there is only a small barrier to back transfer of the hole to the free-base porphyrin to regenerate $(P_{ZP})_3-P_{ZC}-P^{\bullet+}-C_{60}^{\bullet-}$, which can undergo rapid charge recombination. In fact, the lifetime of the final charge-separated state in **1** was only 1.3 ns. In hexad **2**, the first oxidation potential

of the free-base porphyrin has been increased to 1.05 V vs SCE. Migration of the positive charge from the free-base porphyrin of the initially formed $(P_{ZP})_3-P_{ZC}-P^{\bullet+}-C_{60}^{\bullet-}$ state to the zinc porphyrin system to give $((P_{ZP})_3-P_{ZC})^{\bullet+}-P-C_{60}^{\bullet-}$ has a driving force of ~0.26 eV and, in fact, is observed to occur with $k_7 = 2.3 \times 10^9\ s^{-1}$. On the other hand, re-formation of $(P_{ZP})_3-P_{ZC}-P^{\bullet+}-C_{60}^{\bullet-}$ is endergonic by a corresponding amount. Thus, the lifetime of the final charge-separated state is increased to 240 ns.

Conclusions

Through the use of principles of energy transfer and electron-transfer gleaned from theory, from the large body of previous research, and from photosynthesis itself, synthetic antenna−reaction center complex **2** has been optimized to gather light efficiently and use the resulting energy to generate a charge-separated state in high quantum yield. One key design improvement made to hexad **2** compared with hexad **1** stemmed from the recognition that the electronic composition of the porphyrins (frontier molecular orbitals, site of linker connection) is a critical factor in determining the rate of through-bond energy transfer. The only difference between **1** and **2** is that the free-base porphyrin is a β-octaalkylporphyrin in the former while a *meso*-tetraarylporphyrin is used in the latter. The time constant for energy transfer from the core zinc porphyrin to the free-base porphyrin is 244 ps in **1** versus 32 ps in **2**. This 7.6-fold increase in rate causes a significant increase in the overall quantum yield of charge separation, from 0.69 in **1** to 0.98 in **2**.

Another consequence of the change in composition of the free-base porphyrin in the two hexads is that the energetics of the charge-separated state is altered. The free-base tetraarylporphyrin is significantly more resistant toward oxidation than the β-octaalkylporphyrin. Accordingly, in hexad **2**, the hole (formed upon charge separation with the fullerene), which resides on the free-base tetraarylporphyrin, is able to migrate via hole hopping into the antenna comprised of zinc porphyrins; in hexad **1,** the hole on the free-base β-octaalkylporphyrin is apparently not able to do so, at least at a rate competitive with that of charge recombination. The lifetime of the ultimate charge-separated state in **2** is long enough so that the molecule or its relatives would in theory be suitable as components of solar energy conversion or optoelectronic devices. However, the efficiency of **2** still does not approach that of the natural antenna−reaction center complexes, which feature larger antenna arrays and a much higher ratio of antenna chromophores to reaction centers and which harvest light with high efficiency across the entire solar spectrum. Various approaches to increasing the size of the light-harvesting array in biomimetic systems while maintaining high efficiency are being pursued in these and other laboratories.

Experimental Section

Synthesis. The preparations of tetrad **3** and hexad **1** have been reported.[42,45]

*5-(4-Carbomethoxyphenyl)-15-(4-iodophenyl)-10,20-dimesitylporphyrin (**6**).* To follow an early method[63] for synthesis of substituted porphyrins now known to cause only a low level of substituent scrambling,[64] a solution of 2.20 g (8.32 mmol) of 5-mesityldipyrromethane,[63] 0.730 g (4.41 mmol) of methyl 4-formylbenzoate, and 0.910 g (3.91 mmol) of 4-iodobenzaldehyde in 800 mL of $CHCl_3$ was flushed with argon for 20 min. A 1.10 mL portion of 2.5 M $BF_3{\cdot}OEt_2$ in $CHCl_3$ was added dropwise, while the contents were stirred under an argon atmosphere. After 2 h, the red solution was stirred with 2.0 g of 2,3-dichloro-5,6-dicyanobenzoquinone (DDQ) for 16 h at room temperature. Thin layer chromatography (TLC) indicated that oxidation was incomplete. The reaction mixture was diluted with CH_2Cl_2 and washed with aqueous $NaHCO_3$. After evaporation of the solvent, the residue was redissolved in toluene (200 mL) containing 2.0 g of DDQ, and the solution was refluxed for 2 h. The solvent was again evaporated, the residue was dissolved in CH_2Cl_2, and the solution was washed with aqueous $NaHCO_3$. After drying over anhydrous sodium sulfate, the solvent was evaporated, and the residue was chromatographed on silica gel (toluene/0.1−3% ethyl acetate) to give 1.04 g of porphyrin **6** (28% yield): ^{1}H NMR (300 MHz) δ −2.65 (2H, s, NH), 1.83 (12H, s, Ar−CH_3), 2.62 (6H, s, Ar−CH_3), 4.10 (3H, s, $COOCH_3$), 7.28 (4H, s, Ar−H), 7.95 (2H, d, $J = 8$ Hz, Ar−H), 8.08 (2H, d, $J = 8$ Hz, Ar−H), 8.30 (2H, d, $J = 8$ Hz, Ar−H), 8.41 (2H, d, $J = 8$ Hz, Ar−H), 8.69−8.78 (8H, m, β-H); MALDI-TOF-MS *m*/*z* calcd for $C_{52}H_{43}N_4O_2I$ 882, obsd 882; UV/vis (CH_2Cl_2) 418, 516, 550, 592, 650 nm.

*5-(4-Carbomethoxyphenyl)-15-(4-(2-phenylethynyl)phenyl)-10,20-dimesitylporphyrin (**7**).* To a heavy-walled glass tube (40 mL) was added 150 mg (0.17 mmol) of porphyrin (**6**), 20 mL of freshly distilled triethylamine, 37 μL (0.34 mmol) of phenylacetylene, and 83 mg (0.27 mmol) of triphenylarsine. After cooling the suspension to 0 °C, argon was bubbled through the reaction mixture for 20 min, 31 mg (0.034 mmol) of tris(dibenzylideneacetone)dipalladium(0) was added, and the gas flow was continued for an additional 10 min. The tube was sealed (Teflon screw cap), and the reaction mixture was warmed to 45 °C for 24 h. The solvent was evaporated, and the residue was chromatographed on silica gel (CH_2Cl_2/hexanes) to give 130 mg of porphyrin **7** (89% yield): ^{1}H NMR (300 MHz) δ −2.62 (2H, s, NH), 1.84 (12H, s, Ar−CH_3), 2.63 (6H, s, Ar−CH_3), 4.10 (3H, s, $COOCH_3$), 7.28 (4H, s, Ar−H), 7.40−7.47 (3H, m, Ar−H), 7.67−7.70 (2H, m, Ar−H), 7.92 (2H, d, $J = 8$ Hz, Ar−H), 8.23 (2H, d, $J = 8$ Hz, Ar−H), 8.31 (2H, d, $J = 8$ Hz, Ar−H), 8.43 (2H, d, $J = 8$ Hz, Ar−H), 8.70−8.83 (8H, m, β-H); MALDI-TOF-MS *m*/*z* calcd for $C_{60}H_{48}N_4O_2$ 857, obsd 857; UV/vis (CH_2Cl_2) 420, 516, 552, 594, 646 nm.

*5-(4-Formylphenyl)-15-(4-(2-phenylethynyl)phenyl)-10,20-dimesitylporphyrin (**8**).* A flask containing 100 mg (0.12 mmol) of porphyrin **7** and 30 mL of tetrahydrofuran was flushed with nitrogen and cooled to 0 °C. Lithium aluminum hydride (LAH) was added in small portions to the solution such that reduction of the ester to the corresponding alcohol was achieved. Residual LAH was quenched by the addition of ice to the reaction mixture, CH_2Cl_2 (100 mL) was then added, and the mixture was filtered through Celite. The filter cake was washed with CH_2Cl_2/methanol (4:1) until all of the porphyrin had been extracted. The filtrate was then concentrated and dried. Without further purification, the porphyrin alcohol was dissolved in CH_2Cl_2 (40 mL) and subjected to oxidation by activated manganese dioxide. TLC indicated that the conversion of the alcohol to the corresponding aldehyde had occurred, so the reaction mixture was filtered through Celite, and the filtrate was concentrated. This material was then chromatographed on silica gel (CH_2Cl_2/hexanes) to give 92 mg of porphyrin **8** (95% yield): ^{1}H NMR (300 MHz) δ −2.61 (2H, s, NH), 1.84 (12H, s, Ar−CH_3), 2.63 (6H, s, Ar−CH_3), 7.28 (4H, s, Ar−H), 7.40−7.45 (3H, m, Ar−H), 7.67−7.70 (2H, m, Ar−H), 7.92 (2H, d, $J = 8$ Hz, Ar−H), 8.22 (2H, d, $J = 8$ Hz, Ar−H), 8.26 (2H, d, $J = 7$ Hz, Ar−H), 8.41 (2H, d, $J = 7$ Hz, Ar−H), 8.71−8.83 (8H, m, β-H), 10.37 (1H, s, CHO); MALDI-TOF-MS *m*/*z* calcd for $C_{59}H_{46}N_4O$ 827, obsd 827; UV/vis (CH_2Cl_2) 424, 516, 552, 594, 650 nm.

*Porphyrin−C_{60} Dyad (**5**).* To a 60-mL threaded tube was added 75 mg (0.091 mmol) of porphyrin **8**, 50 mL of toluene, 81 mg (0.91 mmol) of sarcosine, and 131 mg (0.18 mmol) of C_{60}. The tube was flushed with argon and then sealed with a Teflon screw cap. The reaction mixture was warmed to 110 °C for 24 h; TLC after this time indicated that most of the porphyrin aldehyde had reacted and a material with little or no fluorescence had formed. The solvent was evaporated, and the residue was redissolved in a mixture of toluene/25% carbon disulfide. This solution was chromatographed on a silica gel column (toluene/0.1% ethyl acetate) to give 77 mg of dyad **5** (54% yield): ^{1}H NMR (300 MHz) δ −2.66 (2H, s, NH), 1.80 (6H, s, Ar−CH_3), 1.82 (6H, s, Ar−CH_3), 2.59 (6H, s, Ar−CH_3), 3.10 (3H, s, N−CH_3), 4.42 (1H, d, J = 9 Hz, pyrrolid-H), 5.09 (1H, d, J = 9 Hz, pyrrolid-H), 5.26 (1H, s, pyrrolid-H), 7.29 (4H, s, Ar−H), 7.36−7.45 (3H, m, Ar−H), 7.63−7.66 (2H, m, Ar−H), 7.89 (2H, d, J = 8 Hz, Ar−H), 8.1−8.3 partially obscured (2H, br s, Ar−H), 8.18 (2H, d, J = 8 Hz, Ar−H), 8.25 (2H, d, J = 7 Hz, Ar−H), 8.62−8.79 (8H, m, β-H); MALDI-TOF-MS *m*/*z* calcd for $C_{121}H_{51}N_5$ 1575, obsd 1576; UV/vis (CH_2Cl_2) 422, 516, 552, 592, 648, 704 nm.

*5-(4-Cyanophenyl)-15-(4-iodophenyl)-10,20-dimesitylporphyrin (**9**).* To follow an early method[63] for synthesis of substituted porphyrins now known to cause only a low level of substituent scrambling,[64] a solution of 2.30 g (8.70 mmol) of 5-mesityldipyrromethane, 0.63 g (4.79 mmol) of 4-cyanobenzaldehyde and 0.91 g (3.92 mmol) of 4-iodobenzaldehyde in 800 mL of $CHCl_3$ was flushed with argon for 20 min prior to the addition of 1.2 mL of 2.5 M BF_3·OEt_2 ($CHCl_3$). Stirring was continued for 2 h at room temperature. The red solution was treated with 2 g of DDQ over a 14 h period, after which time TLC indicated that oxidation was incomplete. The reaction mixture was then refluxed in toluene containing 2 g of DDQ for 2 h. The solvent was evaporated, and the residue was dissolved in CH_2Cl_2. After washing this solution with saturated aqueous $NaHCO_3$, the solvent was once again evaporated, and the residue was chromatographed on silica gel (toluene/10% hexanes/0.1% ethyl acetate). The compound was again chromatographed on silica gel (toluene/25% hexanes/0.1% ethyl acetate) to give 0.58 g of porphyrin **9** (16% yield): ^{1}H NMR (300 MHz) δ −2.66 (2H, s, NH), 1.83 (12H, s, Ar−CH_3), 2.63 (6H, s, Ar−CH_3), 7.29 (4H, s, Ar−H), 7.94 (2H, d, J = 8 Hz, Ar−H), 8.04 (2H, d, J = 8 Hz, Ar−H), 8.08 (2H, d, J = 8 Hz, Ar−H), 8.34 (2H, d, J = 8 Hz, Ar−H), 8.67−8.79 (8H, m, β-H); MALDI-TOF-MS *m*/*z* calcd for $C_{51}H_{40}N_5I$ 850, obsd 850; UV/vis (CH_2Cl_2) 424, 516, 550, 592, 648 nm.

*5-(4-Formylphenyl)-15-(4-iodophenyl)-10,20-dimesitylporphyrin (**10**).* A flask containing 50 mg (0.059 mmol) of porphyrin **9** and 10 mL of tetrahydrofuran was cooled to −78 °C, and to this solution was added 0.6 mL of 1 M Dibal-H (in hexane). The mixture was stirred under a nitrogen atmosphere for 4 h and at room temperature for an additional 12 h. A 10-mL portion of 10% hydrochloric acid was added to the mixture, which was then stirred vigorously for 1 h. The green emulsion was diluted with CH_2Cl_2 (100 mL) and washed with saturated $NaHCO_3$. After evaporating the solvent, the residue was chromatographed on silica gel (CH_2Cl_2) to give 31 mg of porphyrin **10** (62% yield): ^{1}H NMR (300 MHz) δ −2.63 (2H, s, NH), 1.84 (12H, s, Ar−CH_3), 2.64 (6H, s, Ar−CH_3), 7.29 (4H, s, Ar−H), 7.96 (2H, d, J = 8 Hz, Ar−H), 8.10 (2H, d, J = 8 Hz, Ar−H), 8.28 (2H, d, J = 8 Hz, Ar−H), 8.41 (2H, d, J = 8 Hz, Ar−H), 8.71−8.80 (8H, m, β-H), 10.39 (1H, s, CHO); MALDI-TOF-MS *m*/*z* calcd for $C_{51}H_{41}N_4IO$ 853, obsd 854; UV/vis (CH_2Cl_2) 422, 516, 522, 592, 648 nm.

*Pentad **4**.* To a threaded tube was added 47 mg (0.015 mmol) of tetrad **3**, 15 mg (0.018 mmol) of porphyrin **10**, 18 mg (0.058 mmol) of triphenylarsine, and 15 mL of triethylamine. The mixture was flushed with argon for 15 min, 7 mg (0.007 mmol) of tris(dibenzylideneacetone)dipalladium(0) was added, and the mixture flushed with argon for an additional 10 min. The tube was sealed with a Teflon screw cap, and the reaction mixture was warmed to 40 °C for 24 h. The solvent was evaporated, and the residue was chromatographed on silica gel with toluene/15−10% hexanes followed by CH_2Cl_2/hexanes to give 23 mg of pentad **4** (40% yield): ^{1}H NMR (400 MHz) δ −2.56 (2H, s, NH), 1.88 (66H, s, Ar−CH_3), 2.03 (6H, s, Ar−CH_3), 2.63 and 2.65 (33H, overlapping s, Ar−CH_3), 7.28 (6H, s, Ar−H), 7.30 (12H, s, Ar−H), 7.31 (4H, s, Ar−H), 7.90 (2H, s, Ar−H), 8.10 (8H, d, J = 8 Hz, Ar−H), 8.15 (6H, d, J = 8 Hz, Ar−H), 8.27 (2H, d, J = 8 Hz, Ar−H), 8.32 (8H, d, J = 8 Hz, Ar−H), 8.36−8.40 (6H, m, Ar−H), 8.43 (2H, d, J = 8 Hz, Ar−H), 8.73 (12H, s, β-H), 8.75 (4H, s, β-H), 8.78 (2H, d, J = 5 Hz, β-H), 8.83 (6H, d, J = 5 Hz, β-H), 8.93 (2H, d, J = 5 Hz, β-H), 8.96 (8H, d, J = 5 Hz, β-H), 9.11 (2H, d, J = 5 Hz, β-H), 9.14 (4H, s, β-H), 10.35 (1H, s, CHO); MALDI-TOF-MS *m*/*z* cald for $C_{264}H_{204}N_{20}O_1Zn_4$ 3934, obsd 3934; UV/vis (CH_2Cl_2) 422, 430, 518, 552, 592, 650 nm.

*Hexad **2**.* To a reaction tube was added 20 mg (0.005 mmol) of pentad **4**, 7 mg (0.01 mmol) of C_{60}, 5 mg (0.05 mmol) of sarcosine, and 10 mL of toluene. The suspension was flushed with argon, the tube was sealed with a Teflon screw cap, and the reaction mixture was warmed at 110 °C for 19 h. Carbon disulfide (5 mL) was added to the reaction mixture, which was then applied to a silica gel column (toluene/20−10% hexanes) to give 17 mg of hexad **2** (71% yield): ^{1}H NMR (500 MHz) δ −2.60 (2H, s, NH), 1.87 (66H, s, Ar−CH_3), 2.03 (6H, s, Ar−CH_3), 2.62 and 2.64 (33H, overlapping s, Ar−CH_3), 3.13 (3H, s, N−CH_3), 4.41 (1H, d, J = 9 Hz, pyrrolid-H), 5.08 (1H, d, J = 9 Hz, pyrrolid-H), 5.23 (1H, s, pyrrolid-H), 7.28 (22H, s, Ar−H), 7.77 (2H, s, Ar−H), 8.07 (8H, d, J = 8 Hz, Ar−H), 8.13 (8H, d, J = 8 Hz, Ar−H), 8.25−8.31 (10H, m, Ar−H), 8.34−8.38 (6H, m, Ar−H), 8.71 (16H, s, β-H), 8.80 (8H, d, J = 5 Hz, β-H), 8.93 (2H, d, J = 5 Hz, β-H), 8.94 (8H, d, J = 5 Hz, β-H), 9.10 (2H, d, J = 5 Hz, β-H), 9.13 (4H, s, β-H); MALDI-TOF-MS *m*/*z* calcd for $C_{326}H_{209}N_{21}Zn_4$ 4681.6, obsd 4683; FAB-MS *m*/*z* obsd 4681.4; UV/vis (CH_2Cl_2) 422, 430, 516, 552, 592, 652, 712 nm.

Instrumental Techniques. All spectroscopic data were collected at room temperature. The ^{1}H NMR spectra were recorded on Varian Unity spectrometers at 300 or 500 MHz. Samples were dissolved in $CDCl_3$ containing tetramethylsilane as an internal reference. High-resolution mass spectra were obtained on a Kratos MS 50 mass spectrometer operating at 8 eV in FAB mode. Other mass spectra were obtained on a matrix-assisted laser desorption/ionization time-of-flight spectrometer (MALDI-TOF). Ultraviolet−visible ground-state absorption spectra were measured on a Shimadzu UV2100U UV−vis spectrometer.

Steady-state fluorescence emission spectra (corrected) were obtained using a SPEX Fluorolog-2. Excitation was produced by a 450 W xenon lamp and single-grating monochromator. Fluorescence was detected at 90° to the excitation beam via a single-grating monochromator and an R928 photomultiplier tube having S-20 spectral response operating in the single-photon-counting mode.

Fluorescence decay measurements were performed on ∼1 × 10^{-5} M solutions by the time-correlated single-photon-counting method. The excitation source was a cavity-dumped Coherent

700 dye laser pumped by a frequency-doubled Coherent Antares 76s Nd:YAG laser. Fluorescence emission was detected at a magic angle using a single-grating monochromator and microchannel plate photomultiplier (Hamamatsu R2809U-11). The instrument response time was ca. 35−50 ps, as verified by scattering from Ludox AS-40. The spectrometer was controlled by software based on a LabView program from National Instruments.[65]

Nanosecond transient absorption measurements were made with excitation from an Opotek optical parametric oscillator pumped by the third harmonic of a Continuum Surelight Nd:YAG laser. The pulse width was ∼5 ns, and the repetition rate was 10 Hz. The detection portion of the spectrometer has been described elsewhere.[66]

The femtosecond transient absorption apparatus consists of a kilohertz pulsed laser source and a pump−probe optical setup and has been previously described.[42] To determine the number of significant components in the transient absorption data, singular value decomposition analysis[50,51] was carried out using locally written software based on the MatLab 5.0 program (MathWorks, Inc.).[42]

Acknowledgment. This work was supported by grants to D.G., T.A.M., and A.L.M. from the National Science Foundation (Grant CHE-0078835) and to J.S.L. from the Department of Energy, Office of Basic Energy Sciences. FAB mass spectrometric studies were performed by the Midwest Center for Mass Spectrometry, with partial support by the National Science Foundation (Grant DIR9017262). This is publication 502 from the ASU Center for the Study of Early Events in Photosynthesis.

References and Notes

(1) Gust, D.; Moore, T. A.; Moore, A. L. *Acc. Chem. Res.* **2001**, *34*, 40−48.

(2) Gust, D.; Moore, T. A. In *The Porphyrin Handbook*; Kadish, K. M., Smith, K. M., Guilard, R., Eds.; Academic Press: New York, 2000; pp 153−190.

(3) Gust, D.; Moore, T. A.; Moore, A. L. *Acc. Chem. Res.* **1993**, *26*, 198−205.

(4) Gust, D.; Moore, T. A. *Adv. Photochem.* **1991**, *16*, 1−65.

(5) Wasielewski, M. R. *Chem. Rev.* **1992**, *92*, 435−461.

(6) Bixon, M.; Fajer, J.; Feher, G.; Freed, J. H.; Gamliel, D.; Hoff, A. J.; Levanon, H.; Möbius, K.; Nechushtai, R.; Norris, J. R.; Scherz, A.; Sessler, J. L.; Stehlik, D. *Isr. J. Chem.* **1992**, *32*, 449−455.

(7) Asahi, T.; Ohkouchi, M.; Matsusaka, R.; Mataga, N.; Zhang, R. P.; Osuka, A.; Maruyama, K. *J. Am. Chem. Soc.* **1993**, *115*, 5665−5674.

(8) Connolly, J. S.; Bolton, J. R. In *Photoinduced Electron Transfer, Part D*; Fox, M. A., Chanon, M., Eds.; Elsevier: Amsterdam, 1988; pp 303−393.

(9) Sakata, Y.; Imahori, H.; Tsue, H.; Higashida, S.; Akiyama, T.; Yoshizawa, E.; Aoki, M.; Yamada, K.; Hagiwara, K.; Taniguchi, S.; Okada, T. *Pure Appl. Chem.* **1997**, *69*, 1951−1956.

(10) Imahori, H.; Sakata, Y. *Adv. Mater.* **1997**, *9*, 537−546.

(11) Bothner-By, A. A.; Dadok, J.; Johnson, T. E.; Lindsey, J. S. *J. Phys. Chem.* **1996**, *100*, 17551−17557.

(12) Hsiao, J.-S.; Krueger, B. P.; Wagner, R. W.; Johnson, T. E.; Delaney, J. K.; Mauzerall, D. C.; Fleming, G. R.; Lindsey, J. S.; Bocian, D. F.; Donohoe, R. J. *J. Am. Chem. Soc.* **1996**, *118*, 11181−11193.

(13) Li, F.; Gentemann, S.; Kalsbeck, W. A.; Seth, J.; Lindsey, J. S.; Holten, D.; Bocian, D. F. *J. Mater. Chem.* **1997**, *7*, 1245−1262.

(14) Seth, J.; Palaniappan, V.; Johnson, T. E.; Prathapan, S.; Lindsey, J. S.; Bocian, D. F. *J. Am. Chem. Soc.* **1994**, *116*, 10578−10592.

(15) Strachan, J. P.; Gentemann, S.; Seth, J.; Kalsbeck, W. A.; Lindsey, J. S.; Holten, D.; Bocian, D. F. *J. Am. Chem. Soc.* **1997**, *119*, 11191−11201.

(16) Wagner, R. W.; Johnson, T. E.; Lindsey, J. S. *J. Am. Chem. Soc.* **1996**, *118*, 11166−11180.

(17) Van Patten, P.; Shreve, A. P.; Lindsey, J. S.; Donohoe, R. J. *J. Phys. Chem. B* **1998**, *102*, 4209−4216.

(18) Imamura, T.; Fukushima, K. *Coord. Chem. Rev.* **2000**, *198*, 133−156.

(19) Angiolillo, P. J.; Lin, V. S. Y.; Vanderkooi, J. M.; Therien, M. J. *J. Am. Chem. Soc.* **1995**, *117*, 12514−12527.

(20) Aratani, N.; Osuka, A.; Kim, Y. H.; Jeong, D. H.; Kim, D. *Angew. Chem., Int. Ed.* **2000**, *39*, 1458−1462.

(21) Biemans, H. A. M.; Rowan, A. E.; Verhoeven, A.; Vanoppen, P.; Latterini, L.; Foekema, J.; Schenning, A. P. H. J.; Meijer, E. W.; de Schryver, F. C.; Nolte, R. J. M. *J. Am. Chem. Soc.* **1998**, *120*, 11054−11060.

(22) Burrell, A. K.; Officer, D. L.; Reid, D. C. W.; Wild, K. Y. *Angew. Chem., Int. Ed.* **1998**, *37*, 114−117.

(23) Chichak, K.; Branda, N. R. *Chem. Commun.* **1999**, 523−524.

(24) Giribabu, L.; Rao, T. A.; Maiya, B. G. *Inorg. Chem.* **1999**, *38*, 4971−4980.

(25) Hyslop, A. G.; Kellett, M. A.; Iovine, P. M.; Therien, M. J. *J. Am. Chem. Soc.* **1998**, *120*, 12676−12677.

(26) Kim, Y. H.; Cho, H. S.; Kim, D.; Kim, S. K.; Yoshida, N.; Osuka, A. *Synth. Met.* **2001**, *117*, 183−187.

(27) Kim, Y. H.; Jeong, D. H.; Kim, D.; Jeoung, S. C.; Cho, H. S.; Kim, S. K.; Aratani, N.; Osuka, A. *J. Am. Chem. Soc.* **2001**, *123*, 76−86.

(28) Kumble, R.; Palese, S.; Lin, V. S. Y.; Therien, M. J.; Hochstrasser, R. M. *J. Am. Chem. Soc.* **1998**, *120*, 11489−11498.

(29) Kuroda, Y.; Shiraishi, N.; Sugou, K.; Sasaki, K.; Ogoshi, H. *Tetrahedron Lett.* **1998**, *39*, 2993−2996.

(30) Lin, V. S. Y.; Dimagno, S. G.; Therien, M. J. *Science* **1994**, *264*, 1105−1111.

(31) Mak, C. C.; Pomeranc, D.; Montalti, M.; Prodi, L.; Sanders, J. K. M. *Chem. Commun.* **1999**, 1083−1084.

(32) Monti, D.; Venanzi, M.; Mancini, G.; Marotti, F.; La Monica, L.; Boschi, T. *Eur. J. Org. Chem.* **1999**, 1901−1906.

(33) Nakano, A.; Osuka, A.; Yamazaki, I.; Yamazaki, T.; Nishimura, Y. *Angew. Chem., Int. Ed.* **1998**, *37*, 3023−3027.

(34) Ogawa, K.; Kobuke, Y. *Angew. Chem., Int. Ed.* **2000**, *39*, 4070−4073.

(35) Ogawa, T.; Nishimoto, Y.; Yoshida, N.; Ono, N.; Osukua, A. *Chem. Commun.* **1998**, 337−338.

(36) Ohta, N.; Iwaki, Y.; Ito, T.; Yamazaki, I.; Osuka, A. *J. Phys. Chem. B* **1999**, *103*, 11242−11245.

(37) Piet, J. J.; Taylor, P. N.; Wegewijs, B. R.; Anderson, H. L.; Osuka, A.; Warman, J. M. *J. Phys. Chem. B* **2001**, *105*, 97−104.

(38) Shimidzu, T. *Synth. Met.* **1996**, *81*, 235−241.

(39) Wilson, G. S.; Anderson, H. L. *Chem. Commun.* **1999**, 1539−1540.

(40) Wagner, R. W.; Lindsey, J. S. *J. Am. Chem. Soc.* **1994**, *116*, 9759−9760.

(41) Wagner, R. W.; Lindsey, J. S.; Seth, J.; Palaniappan, V.; Bocian, D. F. *J. Am. Chem. Soc.* **1996**, *118*, 3996−3997.

(42) Kuciauskas, D.; Liddell, P. A.; Lin, S.; Johnson, T. E.; Weghorn, S. J.; Lindsey, J. S.; Moore, A. L.; Moore, T. A.; Gust, D. *J. Am. Chem. Soc.* **1999**, *121*, 8604−8614.

(43) Yang, S. I.; Seth, J.; Balasubramanian, T.; Kim, D.; Lindsey, J. S.; Holten, D.; Bocian, D. F. *J. Am. Chem. Soc.* **1999**, *121*, 4008−4018.

(44) Yang, S. I.; Seth, J.; Strachan, J. P.; Gentemann, S.; Kim, D.; Holten, D.; Lindsey, J. S.; Bocian, D. F. *J. Porphyrins Phthalocyanines* **1999**, *3*, 117−147.

(45) del Rosario Benites, M.; Johnson, T. E.; Weghorn, S. J.; Yu, L.; Rao, P. D.; Diers, J. R.; Yang, S. I.; Kirmaier, C.; Bocian, D. F.; Holten, D.; Lindsey, J. S. *J. Mater. Chem.*, **2002**, *12*, 65−80.

(46) Maggini, M.; Scorrano, G.; Prato, M. *J. Am. Chem. Soc.* **1993**, *115*, 9798−9799.

(47) Liang, K.; Farahat, M. S.; Perlstein, J.; Law, K.-Y.; Whitten, D. G. *J. Am. Chem. Soc.* **1997**, *119*, 830−831.

(48) McRae, E. G.; Kasha, M. *Physical Processes in Radiation Biology*; Academic Press: New York, 1964; p 17.

(49) Bahr, J. L.; Kuciauskas, D.; Liddell, P. A.; Moore, A. L.; Moore, T. A.; Gust, D. *J. Photochem. Photobiol.* **2000**, *72*, 598−611.

(50) Golub, G. H.; Reinsch, C. *Numer. Math.* **1970**, *14*, 403−420.

(51) Henry, E. R.; Hofrichter, J. In *Methods in Enzymology*; Ludwig, B., Ed.; Academic Press: San Diego, 1992; p 219.

(52) Luo, C.; Guldi, D. M.; Imahori, H.; Tamaki, K.; Sakata, Y. *J. Am. Chem. Soc.* **2000**, *122*, 6535−6551.

(53) Rodriguez, J.; Kirmaier, C.; Holten, D. *J. Am. Chem. Soc.* **1989**, *111*, 6500−6506.

(54) Williams, R. M.; Zwier, J. M.; Verhoeven, J. W. *J. Am. Chem. Soc.* **1995**, *117*, 4093−4099.

(55) Lammi, R. K.; Ambroise, A.; Balasubramanian, T.; Wagner, R. W.; Bocian, D. F.; Holten, D.; Lindsey, J. S. *J. Am. Chem. Soc.* **2000**, *122*, 7579−7591.

(56) Bonnett, R.; McGarvey, D. J.; Harriman, A.; Land, E. J.; Truscott, T. G.; Winfield, U.-J. *Photochem. Photobiol.* **1988**, *48*, 271−276.

(57) Luo, C.; Fujitsuka, M.; Huang, C.-H.; Ito, O. *Phys. Chem. Chem. Phys.* **1999**, *1*, 2923−2928.

(58) Kuciauskas, D.; Liddell, P. A.; Hung, S.-C.; Lin, S.; Stone, S.; Seely, G. R.; Moore, A. L.; Moore, T. A.; Gust, D. *J. Phys. Chem. B* **1997**, *101*, 429−440.

(59) Noss, L.; Liddell, P. A.; Moore, A. L.; Moore, T. A.; Gust, D. *J. Phys. Chem. B* **1997**, *101*, 458−465.

(60) Gust, D.; Moore, T. A.; Moore, A. L.; Macpherson, A. N.; Lopez, A.; DeGraziano, J. M.; Gouni, I.; Bittersmann, E.; Seely, G. R.; Gao, F.; Nieman, R. A.; Ma, X. C.; Demanche, L. J.; Luttrull, D. K.; Lee, S.-J.; Kerrigan, P. K. *J. Am. Chem. Soc.* **1993**, *115*, 11141−11152.

(61) Gust, D.; Moore, T. A.; Moore, A. L.; Gao, F.; Luttrull, D. K.; DeGraziano, J. M.; Ma, X. C.; Makings, L. R.; Lee, S.-J.; Trier, T. T.; Bittersmann, E.; Seely, G. R.; Woodward, S.; Bensasson, R. V.; Rougée, M.; de Schryver, F. C.; Van der Auweraer, M. *J. Am. Chem. Soc.* **1991**, *113*, 3638−3649.

(62) Seth, J.; Palaniappan, V.; Wagner, R. W.; Johnson, T. E.; Lindsey, J. S.; Bocian, D. F. *J. Am. Chem. Soc.* **1996**, *118*, 11194−11207.

(63) Lee, C.-H.; Lindsey, J. S. *Tetrahedron* **1994**, *50*, 11427−11440.

(64) Littler, B. J.; Ciringh, Y.; Lindsey, J. S. *J. Org. Chem.* **1999**, *64*, 2864−2872.

(65) Gust, D.; Moore, T. A.; Luttrull, D. K.; Seely, G. R.; Bittersmann, E.; Bensasson, R. V.; Rougée, M.; Land, E. J.; de Schryver, F. C.; Van der Auweraer, M. *Photochem. Photobiol.* **1990**, *51*, 419−426.

(66) Davis, F. S.; Nemeth, G. A.; Anjo, D. M.; Makings, L. R.; Gust, D.; Moore, T. A. *Rev. Sci. Instrum.* **1987**, *58*, 1629−1631.